千葉大学学位申請論文

Theranostic approach using nanoparticle drug delivery therapy and in vivo imaging: trial of image-guided photo-dynamic therapy for glioma

（ナノ薬剤送達技術による治療と生体イメージングを融合したセラノスティクス　～脳腫瘍での光線力学治療の試み）

千葉大学千葉大学大学院医学薬学府

先端医学薬学専攻

（主任 ： 岩立　康男　教授）

柴田　さやか

I. INTRODUCTION

"Theranostics" is a new medical concept that combines diagnosis and therapy. In vivo visualization using MRI contrast agents and/or fluorescent probes is useful to assess diseases and therapeutic efficacy. In addition, probes that combine contrast agents and therapeutic molecules can allow "image-guided" precision medicine before, during and after therapy. In our study, we developed LP-iDOPE, which incorporates indocyanine green (ICG) in liposome membranes, and applied it to glioblastoma model rats.

GM

Glioblastoma multiforme (GM) is the most common primary malignant brain tumor. It is known to be highly invasive and intractable. The median survival time of GM patients is only 1-2 years with standard surgery and radiation treatments (DeAngelis, 2001 January 11; Krex et al., 2007). After taking Temozolomide, an oral alkylating agent, the median survival time of GM patients was reported to be 14.6 months in recent clinical trials (Stupp et al., 2005 Mar 10). Another study has reported that 73.5% of patients died within 2 years and the recurrence rate after surgery was 72.2% (Brandes et al., 2009 Mar 10). The high invasiveness and high recurrence rate of GM is a big problem. Extended resection is often performed to completely eliminate tumor cells, but this inevitably scratches the surrounding normal brain tissue (Hasegawa et al., 2010).

ICG

Indocyanine green (ICG), which is a small water-soluble dye know since the 1950's, has an absorption and fluorescence spectrum in the near infrared (NIR) region (600 to 1200 nm). ICG is widely used in biomedical research and clinical applications as a biomarker or a contrast agent in studies involving the heart, liver, lungs and blood circulation due to its biocompatibility (Flower & Hochheimer, 1976 Feb). The use of NIR fluorescence imaging *in vivo* offers the advantage that tissue autofluorescence is very low so that interference is minimized, optimum contrast is easily obtained and deeper penetration of the signal is possible. However, the half-life of ICG in blood is as short as 3-4 minutes, so practical imaging time is around 15 minutes.(Belykh et al., 2016; Cherrick, Stein, Leevy, & Davidson, 1960 Apr)

PTT/PDT

There has been an on-going effort to utilize ICG in conjunction with biomolecules to afford diagnosis, and photothermal therapy (PTT) and photodynamic therapy (PDT) of cancer.(Olzowy et al., 2002 Oct; Quirk et al., 2015)

PTT refers to efforts to use electromagnetic radiation, such as infrared wavelengths, for the treatment of various diseases, including cancer. When the temperature rises between 45°C to 300°C, therapeutic effects can be obtained at sufficient depths using NIR irradiation.

PDT provides additional specificity to therapeutic techniques becanse irradiated light is applied only to the diseased tissue and there is little damage to the surrounding

benign tissue. This spatial specificity and minimal-invasiveness make PTT an attractive therapeutic modality is comparison to open surgery or other invasive therapeutic procedures. PDT is believed to act through cytotoxic singlet oxygen (reactive oxygen species). Singlet oxygen is formed when a photosensitizer is excited by light and transfers its energy to the molecular oxygen in tissues. The oxidization of the singlet oxygen may be the principal way tumor cells are destroyed in PDT.

PEGylated Liposome

Liposomes have promised to be drug carriers for clinical application since the 1970s (Hill & Bangham, 1975). However, simple liposomes have poor blood retention *in vivo* as they are captured in by the reticuloendothelial system (RES). Allen et al. (Allen, Hansen, Martin, Redemann, & Yau-Young, 1991 Jul 1) proposed a modified liposome with polyethylene glycol on the surface (PEGylated Liposome). The PEG on the liposome inhibits albumin adsorption by making the hydration layer thay makes is difficult for to phagocytes recognize. PEGylated liposome has long blood retention and this opens the way for clinical application. Additionally, in the 1980s, Maeda et al. (Maeda, 2015 Aug 30) discovered the enhanced permeability and retention (EPR) effect , where particles of approximately 100-300 nm diameter can accumulate in tumor or inflamed tissues. PEGylated liposomes have a diameter of around 100-300 nm and are therefore expected to accumulate in the tumor while circulating for a long time in the blood stream.

PTT/PDT using ICG conjugated PEGylated Liposome

Our goal is to establish a theranostic application for (1) accumulating PEGylated liposomes carrying ICG to tumors, (2) fluorescent enhancement of the tumor tissue for NIR imaging, and (3) treatment of the tumor with PDT.

Accumulation of PEGylated Liposome in the tumor clarifies the boundary between normal tissue and tumor tissue so that strong imaging contrast can be maintained for longer observation time. In the case of resectional surgery for brain tumor, our system can reduce the damage for normal brain tissue and help more accurate resection. In addition, PDT may prevent tumor recurrence from the boundary of the resection. All of these benefits benefiits lead to minimizing side effects. The ICG conjugated PEGylated Liposome may also increase the effectiveness of brain tumor resection surgery, thus improving the survival rate and quality of life of GM patients.

References

Allen, T., Hansen, C., Martin, F., Redemann, C., & Yau-Young, A. (1991 Jul 1). Liposomes containing synthetic lipid derivatives of poly(ethylene glycol) show prolonged circulation half-lives in vivo. *Biochim Biophys Acta, 1066(1)*, 29-36.

Belykh, E., Martirosyan, N. L., Yagmurlu, K., Miller, E. J., Eschbacher, J. M., Izadyyazdanabadi, M., . . . Preul, M. C. (2016). Intraoperative Fluorescence Imaging for Personalized Brain Tumor Resection: Current State and Future Directions. *Front Surg, 3*, 55. doi:10.3389/fsurg.2016.00055

Brandes, A., Tosoni, A., Franceschi, E., Sotti, G., Frezza, G., Amistà, P., . . . Ermani, M. (2009 Mar 10). Recurrence pattern after temozolomide concomitant with and adjuvant to radiotherapy in newly diagnosed patients with glioblastoma: correlation With MGMT promoter methylation status. *J Clin Oncol, 27(8)*, 1275-1279.

Cherrick, G. R., Stein, S. W., Leevy, C. M., & Davidson, C. S. (1960 Apr). INDOCYANINE GREEN: OBSERVATIONS ON ITS PHYSICAL PROPERTIES, PLASMA DECAY, AND HEPATIC EXTRACTION. *J Clin Invest, 39(4)*, 592–600.

DeAngelis, M. (2001 January 11). Brain Tumors. *N Engl J Med, Vol. 344, No. 2*.

Flower, R., & Hochheimer, B. (1976 Feb). Indocyanine green dye fluorescence and infrared absorption choroidal angiography performed simultaneously with fluorescein angiography. *Johns Hopkins Med J., 138(2)*, 33-42.

Hasegawa, Y., Kinoh, H., Iwadate, Y., Onimaru, M., Ueda, Y., Harada, Y., . . .

Yonemitsu, Y. (2010). Urokinase-targeted fusion by oncolytic Sendai virus eradicates orthotopic glioblastomas by pronounced synergy with interferon-beta gene. *Mol Ther, 18*(10), 1778-1786. doi:10.1038/mt.2010.138

Hill, M., & Bangham, A. (1975). General depressant drug dependency : a biophysical hypothesis. *Adv Exp Med Biol, 59*, 1-9.

Krex, D., Klink, B., Hartmann, C., von Deimling, A., Pietsch, T., Simon, M., . . . German Glioma, N. (2007). Long-term survival with glioblastoma multiforme. *Brain, 130*(Pt 10), 2596-2606. doi:10.1093/brain/awm204

Maeda, H. (2015 Aug 30). Toward a full understanding of the EPR effect in primary and metastatic tumors as well as issues related to its heterogeneity. *Adv Drug Deliv Rev, 91*, 3-6.

Olzowy, B., Hundt, C., Stocker, S., Bise, K., Reulen, H., & Stummer, W. (2002 Oct). Photoirradiation therapy of experimental malignant glioma with 5-aminolevulinic acid. *J Neurosurg, 97(4)*, 970-976.

Quirk, B. J., Brandal, G., Donlon, S., Vera, J. C., Mang, T. S., Foy, A. B., . . . Whelan, H. T. (2015). Photodynamic therapy (PDT) for malignant brain tumors--where do we stand? *Photodiagnosis Photodyn Ther, 12*(3), 530-544. doi:10.1016/j.pdpdt.2015.04.009

Stupp, R., Mason, W., Bent, M., Weller, M., Fisher, B., Taphoorn, M., . . . Group, N. C. I. o. C. C. T. (2005 Mar 10). Radiotherapy plus concomitant and adjuvant temozolomide for glioblastoma. *N Engl J Med, 352(10)*, 987-996.

II. Liposomally formulated phospholipid-conjugated indocyanine green for intra-operative brain tumor detection and resection

Abstract

Some tumor-specific near-infrared (NIR) fluorescent dyes such as indocyanine green (ICG), IDRye800CW, and 5-aminolevulinic acid have been used clinically for detecting tumor margins or micro-cancer lesions. In this study, we evaluated the physicochemical properties of liposomally formulated phospholipid-conjugated ICG, denoted by LP-iDOPE, as a clinically translatable NIR imaging nanoparticle for brain tumors. We also confirmed its brain-tumor-specific biodistribution and its characteristics as the intra-operative NIR imaging nanoparticles for brain tumor surgery. These properties of LP-iDOPE may enable neurosurgeons to achieve more accurate identification and more complete resection of brain tumor.

1. Introduction

Gliomas are the most common type of primary brain tumor and are classified into four categories according to the World Health Organization (WHO) grading system: low-grade (WHO Grade I and II) and high-grade (WHO Grade III and IV). (Kleihues et al.,1993) The complete removal of brain tumor tissues by extended resection is usually hard to perform without injuring surrounding normal brain tissues. (Schucht et al., 2015) It is therefore a challenge for neurosurgeons to remove brain tumor tissues completely by resection; leaving any cancer tissues behind can lower the patient's

quality of life (QOL) and reduce survival times. (Talibi et al., 2014; Tate, 2015) Awide range of clinical applications have been developed in attempts to achieve more complete brain tumor resections (Keunen et al., 2014). However, accurate identification of the tumor region that needs to be resected is still of great importance in brain tumor surgery (Kircher et al., 2012; Jermyn et al., 2015). Over the past decade, intra-operative imaging using near-infrared (NIR) fluores- cence techniques has entered the surgical theatre to fill the gap between pre-operative imaging and intra-operative reality (Vahr-meijer et al., 2013; de Boer et al., 2015). Some tumor-specific NIR fluorescent dyes have been approved for clinical tumor imaging: indocyanine green (ICG) has been used as a targeted free NIR dye for micro-cancer imaging and breast cancer assisted sentinel lymph node mapping; IRDye800CW, conjugated with antibody targeting VEGF-bevacizumab (VEGF: vascular endothelial growth factor) has completed preclinical toxicity studies, and is currently undergoing clinical trials as a NIR dye conjugate for early cancer detection; 5-aminolevulinic acid, preferentially taken up by tumor cells leading to biosynthesis and accumulation of protoporphyrin IX, has been approved in Germany and Japan as an activatable NIR dye for imaging malignant gliomas (Luo et al., 2011; Keereweer et al., 2013; Swanson et al., 2015).

Intravenous injection of ICG was approved by the Food and Drug Administration in the 1950s for several clinical applications and has been shown to have a low negative-reaction profile (Dzurinko et al., 2004). The first application of ICG for macroscopic demarcation of brain tumor margins was investigated in 1993 (Hansen et al., 1993). However, this technique is not effective in distinguishing between tumor

regions and normal regions of the brain that may incidentally uptake the injected dye (Tamura et al., 2012). Cellular visualization using ICG as a contrast agent is therefore needed to overcome these limitations. The investigation of potential imaging techniques in the field of brain tumor surgery, and the development of new imaging dyes and accommodated devices that are available during brain tumor surgery are therefore important (Zehri et al., 2014). In this study, we attempted to improve the specificity and sensitivity of brain tumor imaging using an ICG fluorophore (Murahari and Yergeri, 2013). We previously developed a novel NIR fluorescent probe in which an ICG fluorophore is covalently conjugated with 1,2-dioleoyl-sn-glycero-3-phosphoethanolamine (DOPE), denoted by iDOPE, for incorporation into liposome bilayers as liposomally formulated iDOPE (LP-iDOPE) (Suganami et al., 2012). We then evaluated the characteristics of LP-iDOPE as a clinically translatable fluorescent nanoparticle for brain tumors, based on the enhanced permeability and retention (EPR) effect, and as a NIR fluorescent dye for intra-operative identification of brain tumors. We presume that LP-iDOPE is potentially of great value as a NIR fluorescence image-guidance intra-operative dye, which could make a clear demarcation at brain tumor borders.

2. Material and methods

iDOPE was prepared as previously reported (Suganami et al., 2012). Cholesterol ($1.0x10^{-3}$ M, Nippon Fine Chemical Co., Ltd., Tokyo, Japan), 1,2-dioleoyl-sn-glycero-3-phosphocholine (DOPC, $7.5x10^{-3}$ M, NOF Corporation, Tokyo, Japan), N-(carbonyl- methoxypolyethyleneglycol 5000)-1,2-distearoly-sn-glycero-3- phosphoethanolamine sodium salt (DSPE-PEG, 0.5 mM, NOF Corporation), and iDOPE (2.5×10^{-3}M, iDOPE/DOPC molar ratio of 1/3) were dissolved in a mixed organic solvent consisting of CH3OH/CHCl3 (volume ratio: 1/9). A thin lipid film was formed by removal of the solvent under reduced pressure. After addition of an aqueous buffered solution (phosphate buffered saline [PBS], pH 7.4) at room temperature, the liposome dispersion was filtered through a 0.1-mm pore polycarbonate filter attached to a LiposoFast-Stabilizer (Avestin Inc., Ottawa, Canada).

2.2. Molecular modeling

The three-dimensional structure of ICG was constructed using MOE (version 2009, CCG Inc., Montreal, Canada) according to PubChem Compound CID 11967809 (National Center for Biotechnology Information, Bethesda MD, USA). The three-dimensional structure of DOPE was constructed using VMD (http://www.ks.unic.edu/). The three-dimensional structures of ICG and DOPE were used to construct that of iDOPE using the build command in MOE. Molecular mechanics calculations were performed to obtain the local minimum structures of partial membrane region of LP-iDOPE, containing DOPC and iDOPE, using the AMBER99 force field in MOE.

2.3. Measurement of particle size

Particle size analysis of LP-iDOPE was performed using dynamic light-scattering measurements (SZ-100, HORIBA Ltd., Kyoto, Japan).

2.4. UV–vis–NIR and fluorescence spectroscopy

The absorption spectra of LP-iDOPE and ICG dissolved in an aqueous buffered solution [phosphate buffered saline (PBS), pH 7.4] at room temperature were obtained using a UV–vis–NIR spectrometer (UV-3500, Shimadzu, Kyoto, Japan). Fluorescence emissions from LP-iDOPE and ICG dissolved in an aqueous buffered solution (PBS, pH 7.4) at room temperature were observed using a fluorescence spectrometer (F-4500, Hitachi, Tokyo, Japan).

2.5. Animals

All animal procedures were approved by the Institutional Animal Care and Use Committee of Chiba University and the National Institute of Radiological Sciences. Male 7- to 8-week-old Fisher 344 rats were obtained from the Japan SLC, Inc. (Hama-matsu, Japan). Orthotopic glioma model of 9L-L/R cells in rats: A density of $5x10^5$ 9L-L/R cells with 10μL PBS were injected into rat brains using a microinjector (Harvard Apparatus, South Natick, MA, USA). Briefly, the rats were anesthetized with 2.0% isoflurane (Abbott Japan, Tokyo, Japan) and placed in a stereotactic apparatus. A burr hole was made at an appropriate location (1 mm posterior to the bregma and 3 mm right of the midline). A 25-gauge needle was inserted at a point 3 mm ventral from the

dura. These experiments were also done in accordance with the recommendations for the proper care and use of laboratory animals and according to The Law No. 105 and Notification No. 6 of the Japanese Government.

2.6. MRI

All rats were anesthetized with 2.0% isoflurane (Abbott Japan, Tokyo, Japan) and administrated with 0.4 ml of Gd-DTPA (Meglu-mine Gadopentetate, 0.002 ml/g, 50 mmol/l, Bayer, Leverkusen, Germany) intraperitoneally 15 min before MRI measurements. All MRI experiments were performed using a 7.0T horizontal MRI scanner (Magnet: Kobelco and JASTEC, Kobe, Japan; Console: Bruker Biospin, Ettlingen, Germany), with a volume coil for transmission (Bruker Biospin) and an eight-channel phased array surface coil for reception (Rapid Biomedical, Rimpar, Germany). Multi-slice T1-weighted MR images covering the entire brain (T1WI; multi-slice spin echo, TR/TE = 400/9.57 ms, slice thickness = 1.0 mm, slice gap = 0, number of slices = 16, matrix = 256 x 256, field of view = 25.6 x 25.6 mm2, average = 4) were acquired. The slice orientation was trans, axial for all scans. Image reconstruction and analysis were performed using ParaVision (Bruker Biospin).

2.7. NIR fluorescence imaging

The biodistribution of LP-iDOPE was studied by intravenously injecting LP-iDOPE, containing 14.0 mg/kg of LP-iDOPE, through a tail vein of Fisher 344 rats bearing 9L-L/R cells and imaged at 1 day and 7 days after injection, using an In-Vivo MS FX

PRO imaging system (Carestream Health, New York, NY, USA).

3. Results and discussion

3.1. Preparation of LP-iDOPE

As part of our on-going research for the development of multi-purpose NIR fluorescent liposomes for optical imaging and nanoparticle drug carriers, we rationally designed a novel NIR fluorescence probe in which an ICG fluorophore is covalently conjugated with DOPE, i.e., iDOPE, for incorporation into liposome bilayers (Suganami et al., 2012). As shown in Fig. 1a, we speculate that iDOPE infiltrates the lipid membrane by incorporating into 1,2-dioleoyl-sn-glycero-3-phosphocholine (DOPC). In this study, we selected 10 mol% iDOPE (iDOPE/DOPC molar ratio of 1/10) to achieve a high fluorescence intensity by preventing the fluores-cence quenching between neighboring iDOPE species (Namiki et al., 2011). The average LP-iDOPE diameter should usually be controlled to 100–300 nm in consideration of the EPR effect (Maeda, 2015). To confirm that the standard of the EPR effect was met, we filtered the liposome dispersion [iDOPE, DOPC, Cholester- ol, and poly ethylene glycol (PEG)] through a 100 nm pore polycarbonate filter (Hua et al., 2012). Dynamic light-scattering measurements showed that the average LP-iDOPE size was 191 nm (n = 3) (Fig.1b), which satisfies the restriction of the EPR effect. This exceeded size, around 90 nm, is due to the modification of liposome bilayers with iDOPE and PEG, for a “stealth effect”, as shown in Fig. 1a (Ulrich, 2002).

3.2. Physicochemical properties of LP-iDOPE

In the past decade, many clinical studies have shown that NIR fluorescence imaging during brain tumor surgery is feasible (Zehri et al., 2014; Schaafsma et al., 2011). First, to evaluate the properties of LP-iDOPE as a NIR fluorescent liposome, we recorded its NIR fluorescence excitation and emission spectra. As shown in Fig. 2, the lmax excitation (>780 nm) and lmax emission (811 nm) values of LP-iDOPE shifted to longer wave- length than those of ICG (lmax excitation: >780 nm, lmax emission: 800 nm). We presumed that these phenomena were caused by the liposomal formulation of iDOPE, which restricts free movement of the ICG fluorophore and induces a red shift (11 nm) of the lmax emission of LP-iDOPE compared with that of ICG (Schaafsma et al., 2011). The fluorescence intensity of LP- iDOPE (lmax emission: 811 nm) was about 15% higher than that of ICG (lmax emission: 800 nm). In this case, we speculated that restriction of the ICG fluorophore movement by the liposomally formulation converted kinetic energies to fluorescence intensities (Proulx et al., 2010). Based on these results, we assumed that the optical properties of LP-iDOPE as a NIR fluorescence-imaging dye are nearly the same as those of ICG (Figs. S1 and S2 in Supporting information). We therefore concluded that intra-operative NIR- accommodated devices such as pde-neo (HAMAMATSU, Japan), HyperEye Medical System (MIZUHO, Japan), and SPY Intra-operative Imaging System (NOVADAQ, USA), which are based on intra-operative fluorescence imaging techniques using ICG, could be applied in brain tumor surgery, using LP-iDOPE, without any regulation changes.

3.3. Tumor-specific localization of LP-iDOPE: magnetic resonance imaging (MRI) and NIR

As described above, NIR fluorescence image-guided intra-operative techniques using ICG and NIR-accommodated devices have already entered the surgical theatre (Zehri et al., 2014; Schaafsma et al., 2011). We therefore evaluated LP-iDOPE as a new intra-operative nano-imaging agent. First, to estimate the in vivo biodistribution of LP-iDOPE in a brain tumor, we prepared 9L rat glioma cell implantation models. On 7 days after implantation, we followed the brain tumor growth using 7T-MRI, and then injected LP-iDOPE intravenously through the rat tail vein. Next, we performed consecutive NIR fluorescence imaging 1 day and 7 days after injection with LP-iDOPE. As shown in Fig. 3, we observed specific accumulation of LP-iDOPE in the brain tumor, by comparing the tumor position in the MRI (pre-operation) with that in the NIR (intra-operation). We speculate that breakdown of the blood-brain barrier (BBB) in the brain tumor and the EPR effect allows LP-iDOPE to concentrate in the tumor region 1 day after injection with LP-iDOPE (Bhaskar et al., 2010). In contrast, the fluorescence intensity of LP-iDOPE completely disappeared from the tumor region 7 days after injection with LP-iDOPE (Jain and Stylianopoulos, 2010). Additionally, to confirm the accumulation of LP-iDOPE into the reticuloendothelial system, we performed the ex vivo NIR fluorescence imaging for the lung, liver, spleen, and kidneys (Fig. S3 in Supporting information). It is evident that LP- iDOPE accumulates specifically into the brain tumor at 1 day after injection. After 7 days, the accumulation of NIR in all tissues and in the tumor decreased. The key in tumor imaging is to improve the specificity and

to distinguish tumors from normal tissues. Fig. 4 shows tumor-specific localization of LP-iDOPE and creates a “white stars in a black sky” _effect (Vahrmeijer et al., 2013). We were therefore able to identify the structures that need to be resected in brain tumor surgery. In addition, to assess the use of LP-iDOPE in intra-operative surgical resection, we determined the tumor to normal (T/N) ratio. To take examples discussed in the T/N ratio in brain tumors, those of 5-ALA and IRDye 800CW-conjugated RGD peptide which integrin b3 recognizes was 5 hold and 16–80 hold (reflecting the different expression levels of integrin b3 in brain tumors), respectively (Swanson et al., 2015; Huang et al., 2012). Therefore, as shown in Fig. 5, the signal intensity and the T/N ratio of LP-iDOPE (16.3 hold, n = 2) is sufficient for in vivo brain tumor imaging and for assisting neurosurgeons with accurate resection of brain tumors. The accumulation of LP-iDOPE on the brain tumor region was high compared with other organs, such as liver, spleen, and kidneys due to the breakdown of BBB (Fig. 5). On the other hand, the accumulation of LP-iDOPE on the brain normal region was extremely low due to the normal BBB at that region (Fig. 5). Finally, based on a combination of our results and those of previous clinical trials on ICG fluorescence-guided tumor surgery, we propose a protocol using LP-iDOPE: (i) injection of LP-iDOPE 1 day before the operation; (ii) resection of the brain tumor region, with a few margins, under irradiation at the excitation value of LP-iDOPE (around 780 nm) using a light-emitting diode (LED) device; (iii) irradiation at the absorption value of LP-iDOPE (around 810 nm) on a few remaining tumor margins using a LED device to induce cancer cell death with photodynamic therapy (PDT) (Onoyama et al., 2014; Yi et al., 2014), and (iv)

noninvasive irradiation from the skull at the absorption value of LP-iDOPE (around 810 nm) using a LED device to delay or reduce the risk of cancer recurrence (Fig. S4 in Supporting information). We suggest that this protocol permits the intra-operative image-guided brain tumor surgery (Fig. 6a) and the PDT-guided tumor cell death in brain tumor marginal regions remaining after surgery (Fig. 6b). Furthermore, the post-operative PDT treatment in terms of noninvasion may be

useful for post-operative aftercare (Fig. S4 in Supporting informa-tion). This combination of LP-iDOPE with NIR fluorescence (detection and resection) and a beam (PDT) system enables maximum safety in removal of the brain tumor.

4. Conclusions

In this study, we evaluated the use of liposomally formulated phospholipid-conjugated ICG, denoted by LP-iDOPE, as clinically translatable fluorescent nanoparticles for brain tumor surgery. We examined the characteristics of LP-iDOPE relevant to its use as a NIR fluorescence imaging dye, such as its optical properties, particle size, and tumor-specific localization. LP-iDOPE imaging with MRI and a NIR fluorescence imager, with LP-iDOPE injection 1day before surgery, effectively fills the gap between pre-operative imaging and intra-operative reality in detecting tumor and normal brain tissues. Therefore, the use of LP-iDOPE for brain tumor surgery may have the potential to overcome the limitations of traditional intra-operative brain tumor surgery, by highlighting tumor borders in real time and enabling treatment of surgically remaining cancer cells with PDT. In addition, the combination of LP-iDOPE with a LED device in

terms of noninvasive treatment may useful for post-operative aftercare of brain tumor surgery (Fig. S4 in Supporting information). Finally, NIR fluorescence image-guidance of brain tumor surgery with LP-iDOPE will improve patient management by demarcating tumor borders clearly in real time, in terms of the efficiency of brain tumor resections, improvement of QOL, and elongation of survival times (Butte et al., 2014; Barone et al., 2014).

Funding

This work was partly supported by Grants-in-Aid for Scientific Research (No. 25460328 to AS), Ministry of Education, Culture, Sports, Science and Technology, Japan.

Acknowledgments

The authors thank Dr. Gustavo Bajotto of the Strategic Marketing Division of SCRUM Inc. and Dr. Tetsuro Maruyama of Frontier Surgery of Chiba University for the NIR fluorescence imaging measurements. They also thank Ms. Yoko Shinozaki of the Research and Development Division of HORIBA, Ltd. for the dynamic light-scattering measurements and Ms. Aiko Sekita, Mr. Nobuhiro Nitta, and Mr. Yoshikazu Ozawa of Molecular Imaging Center, National Institute of Radiological Sciences for their technical assistance with MRI measurements.

Fifures, Table & Scheme

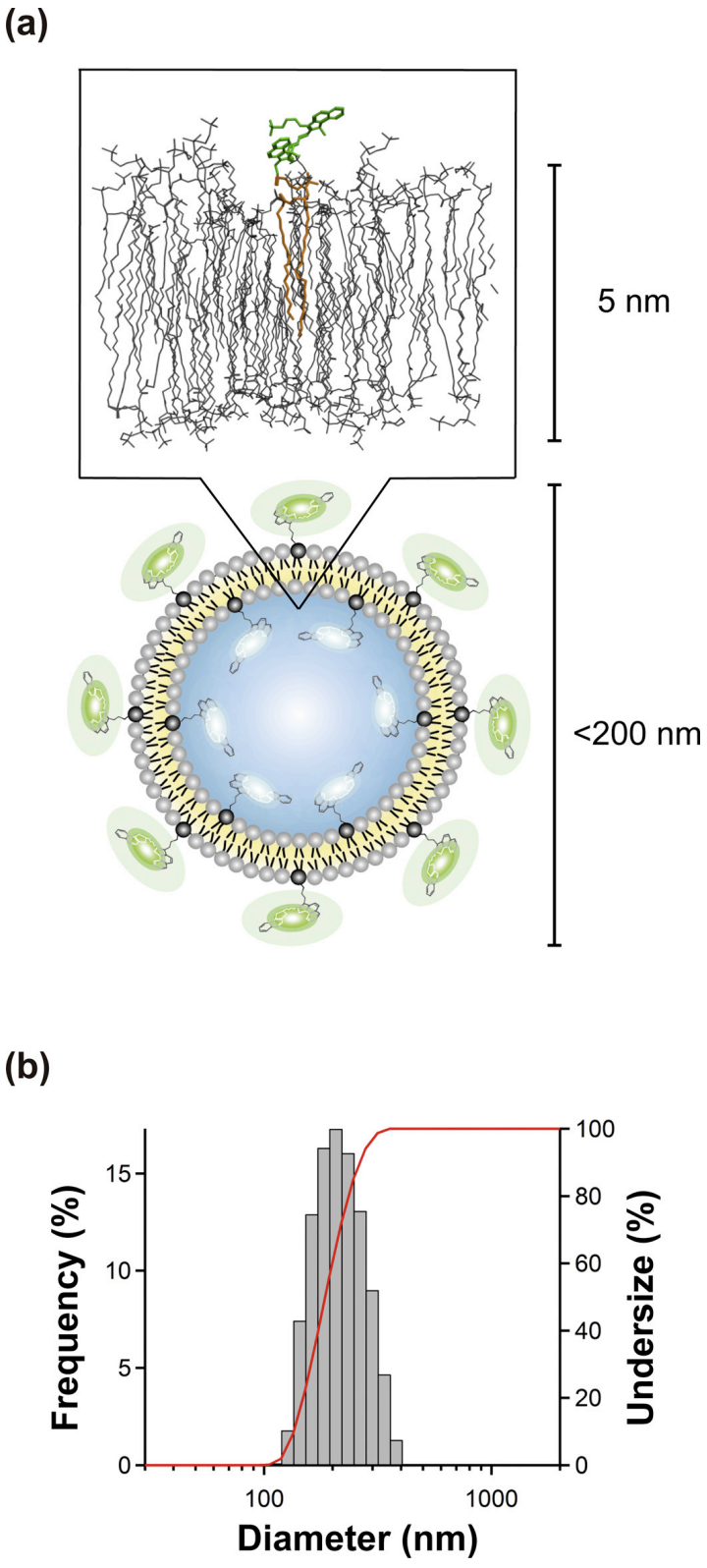

Fig. 1. (a) Schematic and partial membrane structure of LP-iDOPE. Partial membrane structure of LP-iDOPE without cholesterol and PEG: gray, DOPC; green, ICG fluorophore of iDOPE; and orange, DOPE region of iDOPE. (b) Averaged volume of LP-iDOPE. Diameter distribution of LP-iDOPE. iDOPE/DOPC molar ratio was 0.1 (10 mol% iDOPE). Gray bars are differential frequency and red line is cumulative frequency.

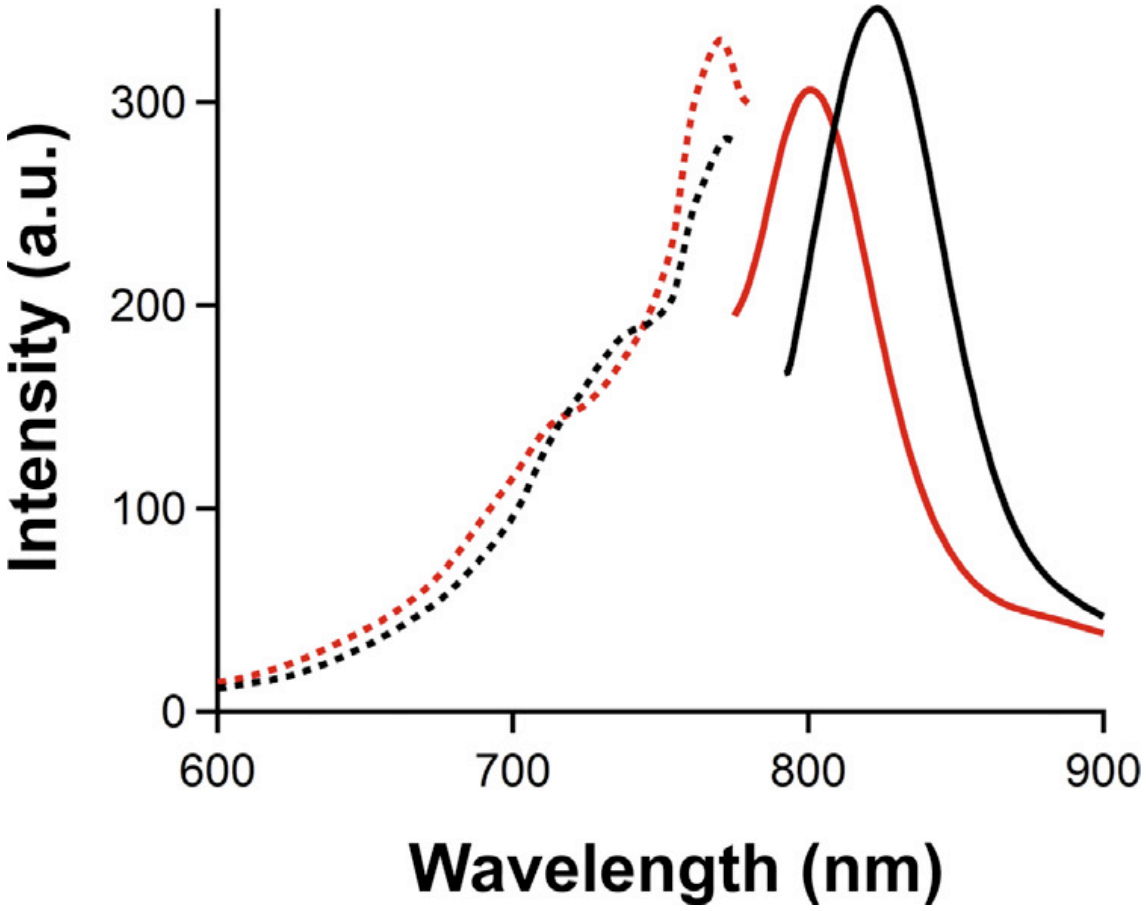

Fig. 2. Optical excitation (dashed line) and emission (full line) of the ICG fluorophore. Normalized vis-NIR absorption spectra of LP-iDOPE (black) and ICG (red) in PBS. Concentrations of the ICG fluorophore of LP-iDOPE and ICG were 1 mM.

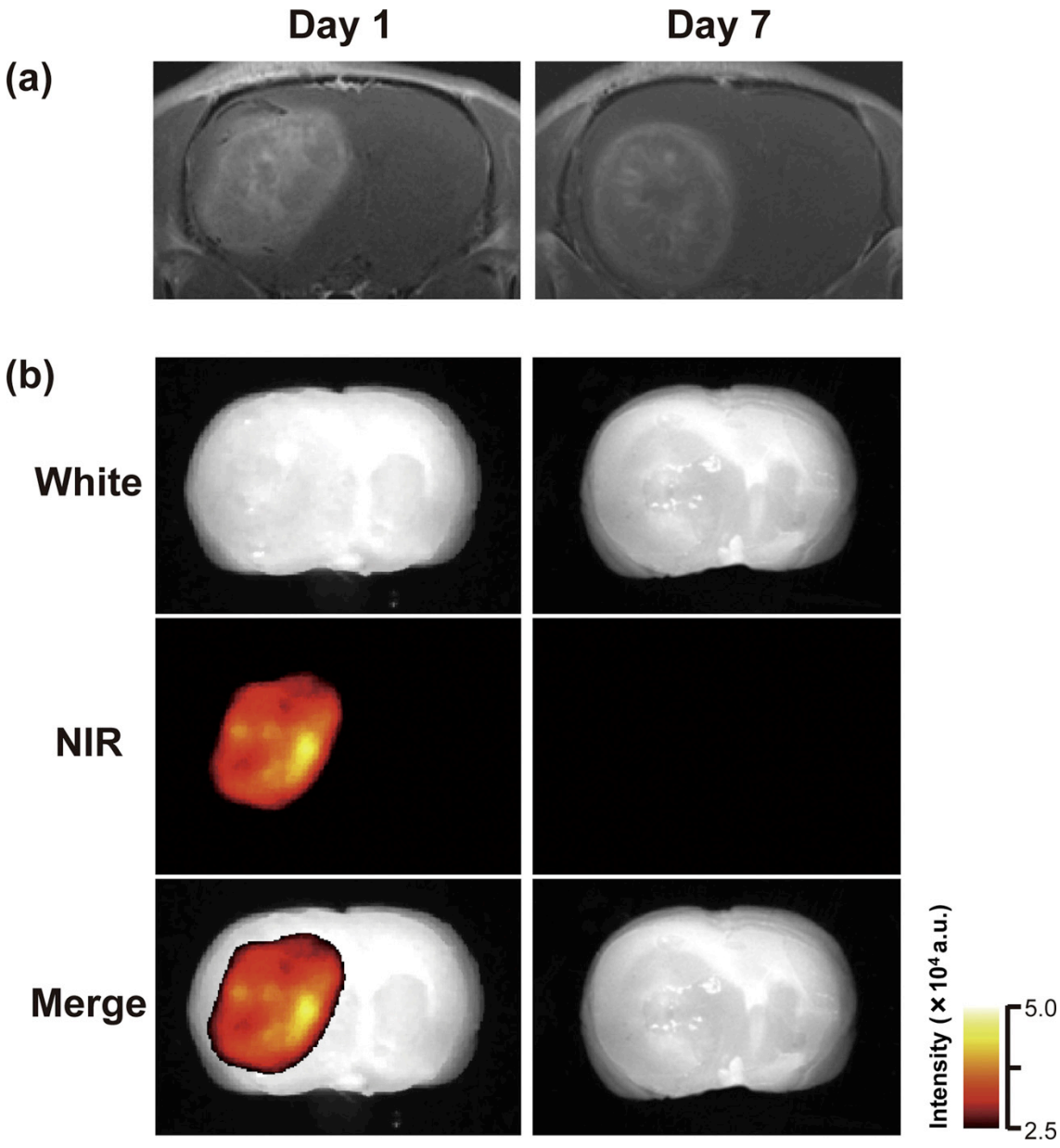

Fig. 3. (a) in vivo MRI and (b) ex vivo NIR fluorescence imaging. Longitudinal observation MRI and NIR fluorescence images of rat bearing 9L tumors: day 1 and day 7 after intravenous injection with LP-iDOPE.

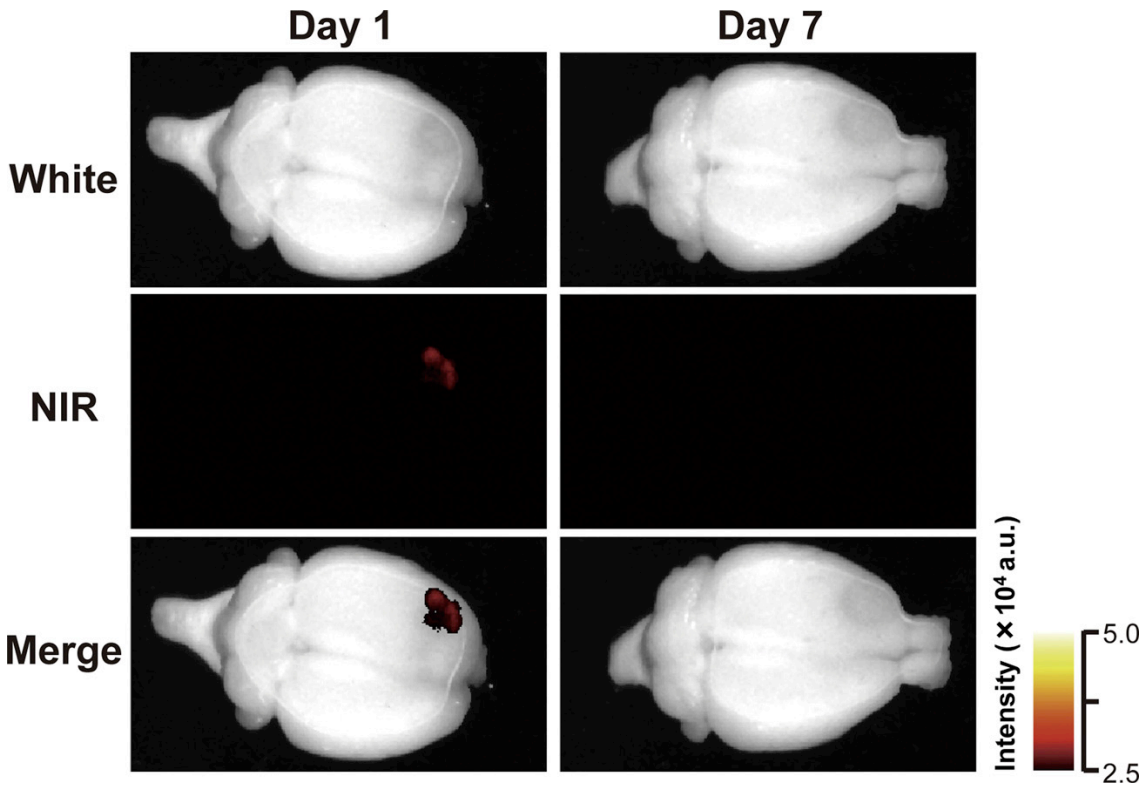

Fig. 4. Ex vivo NIR fluorescence imaging of brain surface. Longitudinal observation NIR fluorescence images of rat bearing 9L tumors: day 1 and day 7 after intravenous injections with LP-iDOPE.

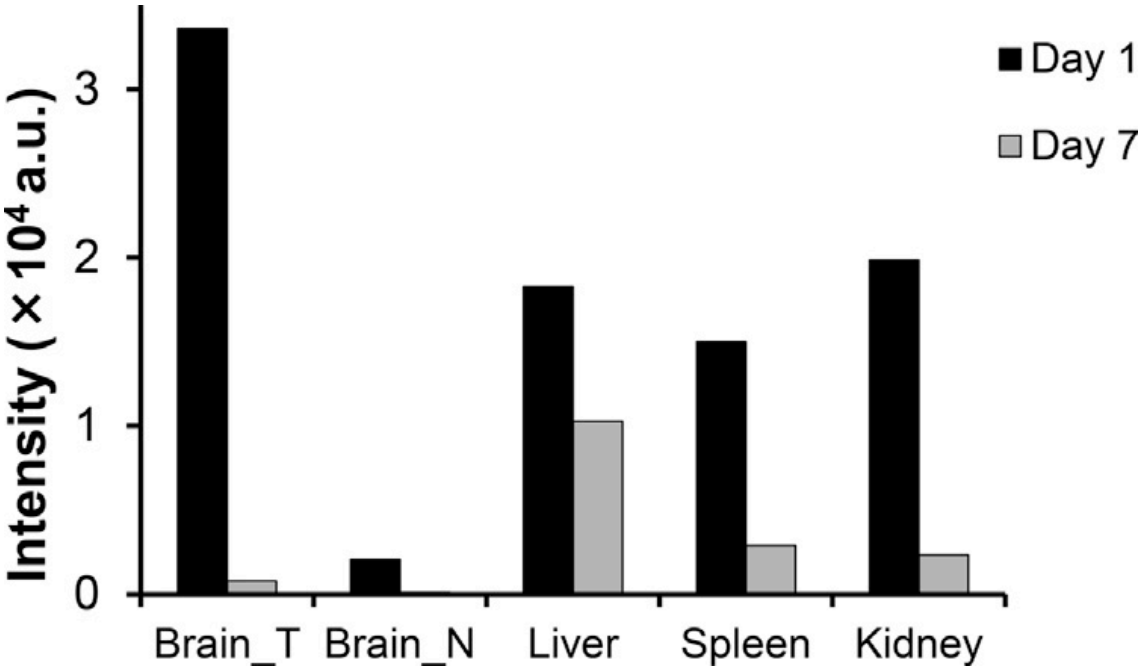

Fig. 5. Longitudinal observation NIR fluorescence intensity of LP-iDOPE in brain, liver, spleen, and kidney of rat bearing 9L tumors: day 1 (black) and day 7 (gray) after intravenous injection with LP-iDOPE (n = 2). Brain_T: tumor region of brain, Brain_N: normal region of brain.

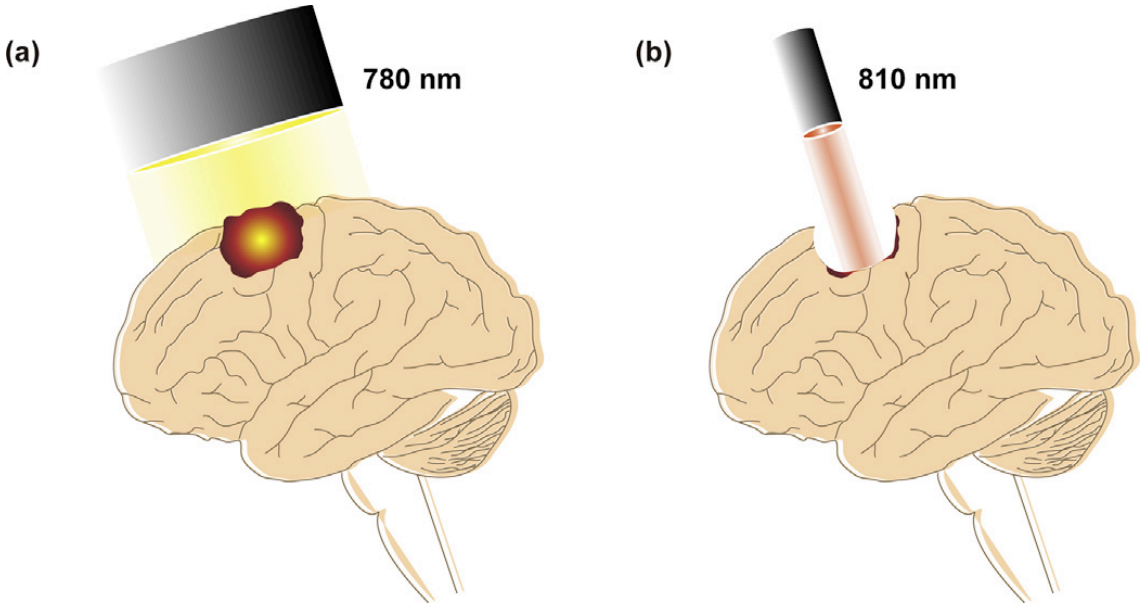

Fig. 6. ICG fluorescence guided tumor surgery. (a) Intra-operative irradiation at excitation value of LP-iDOPE (around 780 nm) to detect brain tumor using LED device and (b) post-resection irradiation at absorption value of LP-iDOPE (around 810 nm) emitted from a LED device to induce cancer cell death by PDT on brain tumor marginal region remaining after surgery.

References

Barone, D.G., Lawrie, T.A., Hart, M.G., 2014. Image guided surgery for the resection of brain tumours. Cochrane Database Syst. Rev. 1, CD009685.

Bhaskar, S., Tian, F., Stoeger, T., Kreyling, W., de la Fuente, J.M., Grazu, V., Borm, P., Estrada, G., Ntziachristos, V., Razansky, D., 2010. Multifunctional Nanocarriers for diagnostics, drug delivery and targeted treatment across blood-brain barrier: perspectives on tracking and neuroimaging. Part. Fibre Toxicol. 7, 3.

Butte, P.V., Mamelak, A., Parrish-Novak, J., Drazin, D., Shweikeh, F., Gangalum, P.R., Chesnokova, A., Ljubimova, J.Y., Black, K., 2014. Near-infrared imaging of brain tumors using the Tumor Paint BLZ-100 to achieve near-complete resection of brain tumors. Neurosurg. Focus 36, E1.

de Boer, E., Harlaar, N.J., Taruttis, A., Nagengast, W.B., Rosenthal, E.L., Ntziachristos, V., van Dam, G.M., 2015. Optical innovations in surgery. Br. J. Surg. 102, e56–72.

Dzurinko, V.L., Gurwood, A.S., Price, J.R., 2004. Intravenous and indocyanine green angiography. Optometry 75, 743–755.

Hansen, D.A., Spence, A.M., Carski, T., Berger, M.S., 1993. Indocyanine green (ICG) staining and demarcation of tumor margins in a rat glioma model. Surg. Neurol. 40, 451–456.

Hua, J., Gross, N., Schulze, B., Michaelis, U., Bohnenkamp, H., Guenzi, E., Hansen, L.L., Martin, G., Agostini, H.T., 2012. In vivo imaging of choroidal angiogenesis using fluorescence-labeled cationic liposomes. Mol. Vis. 18, 1045–1054.

Huang, R., Vider, J., Kovar, J.L., Olive, D.M., Mellinghoff, I.K., Mayer-Kuckuk, P.,

Kircher, M.F., Blasberg, R.G., 2012. Integrin alphavbeta3-targeted IRDye 800CW near-infrared imaging of glioblastoma. Clin. Cancer Res. 18, 5731–5740.

Jain, R.K., Stylianopoulos, T., 2010. Delivering nanomedicine to solid tumors. Nat. Rev. Clin. Oncol. 7, 653–664.

Jermyn, M., Mok, K., Mercier, J., Desroches, J., Pichette, J., Saint-Arnaud, K., Bernstein, L., Guiot, M.C., Petrecca, K., Leblond, F., 2015. Intraoperative brain cancer detection with Raman spectroscopy in humans. Sci. Transl. Med. 7, 274ra219.

Keereweer, S., Van Driel, P.B., Snoeks, T.J., Kerrebijn, J.D., Baatenburg de Jong, R.J., Vahrmeijer, A.L., Sterenborg, H.J., Lowik, C.W., 2013. Optical image-guided cancer surgery: challenges and limitations. Clin. Cancer Res. 19, 3745–3754.

Keunen, O., Taxt, T., Gruner, R., Lund-Johansen, M., Tonn, J.C., Pavlin, T., Bjerkvig, R., Niclou, S.P., Thorsen, F., 2014. Multimodal imaging of gliomas in the context of evolving cellular and molecular therapies. Adv. Drug Deliv. Rev. 76, 98–115.

Kircher, M.F., de la Zerda, A., Jokerst, J.V., Zavaleta, C.L., Kempen, P.J., Mittra, E., Pitter, K., Huang, R., Campos, C., Habte, F., Sinclair, R., Brennan, C.W., Mellinghoff, I.K., Holland, E.C., Gambhir, S.S., 2012. A brain tumor molecular imaging strategy using a new triple-modality MRI-photoacoustic-Raman nanoparticle. Nat. Med. 18, 829–834.

Kleihues, P., Burger, P.C., Scheithauer, B.W., 1993. The new WHO classification of brain tumours. Brain Pathol. 3, 255–268.

Luo, S., Zhang, E., Su, Y., Cheng, T., Shi, C., 2011. A review of NIR dyes in cancer

targeting and imaging. Biomaterials 32, 7127–7138.

Maeda, H., 2015. Toward a full understanding of the EPR effect in primary and metastatic tumors as well as issues related to its heterogeneity. Adv. Drug Deliv. Rev. 2015 (Jan 9) S0169-409X(15) 00004-6.

Murahari, M.S., Yergeri, M.C., 2013. Identification and usage of fluorescent probes as nanoparticle contrast agents in detecting cancer. Curr. Pharm. Des. 19, 4622–_4640.

Namiki, Y., Fuchigami, T., Tada, N., Kawamura, R., Matsunuma, S., Kitamoto, Y., Nakagawa, M., 2011. Nanomedicine for cancer: lipid-based nanostructures for drug delivery and monitoring. Acc. Chem. Res. 44, 1080–1093.

Onoyama, M., Tsuka, T., Imagawa, T., Osaki, T., Minami, S., Azuma, K., Kawashima, K., Ishi, H., Takayama, T., Ogawa, N., Okamoto, Y., 2014. Photodynamic hyperthermal chemotherapy with indocyanine green: a novel cancer therapy for 16 cases of malignant soft tissue sarcoma. J. Vet. Sci. 15, 117–123.

Proulx, S.T., Luciani, P., Derzsi, S., Rinderknecht, M., Mumprecht, V., Leroux, J.C., Detmar, M., 2010. Quantitative imaging of lymphatic function with liposomal indocyanine green. Cancer Res. 70, 7053–7062.

Schaafsma, B.E., Mieog, J.S., Hutteman, M., van der Vorst, J.R., Kuppen, P.J., Lowik, C. W., Frangioni, J.V., van de Velde, C.J., Vahrmeijer, A.L., 2011. The clinical use of indocyanine green as a near-infrared fluorescent contrast agent for image-guided oncologic surgery. J. Surg. Oncol. 104, 323–332.

Schucht, P., Beck, J., Seidel, K., Raabe, A., 2015. Extending resection and preserving

function: modern concepts of glioma surgery. Swiss Med. Wkly. 145, w14082.

Suganami, A., Toyota, T., Okazaki, S., Saito, K., Miyamoto, K., Akutsu, Y., Kawahira, H., Aoki, A., Muraki, Y., Madono, T., Hayashi, H., Matsubara, H., Omatsu, T., Shirasawa, H., Tamura, Y., 2012. Preparation and characterization of phospholipid-conjugated indocyanine green as a near-infrared probe. Bioorg. Med. Chem. Lett. 22, 7481–7485.

Swanson, K.I., Clark, P.A., Zhang, R.R., Kandela, I.K., Farhoud, M., Weichert, J.P., Kuo, J. S., 2015. Fluorescent cancer-selective alkylphosphocholine analogs for intraoperative glioma detection. Neurosurgery 76, 115–123 discussion 123–114.

Talibi, S.S., Talibi, S.S., Aweid, B., Aweid, O., 2014. Prospective therapies for high-grade glial tumours: a literature review. Ann. Med. Surg. 3, 55–59.

Tamura, Y., Hirota, Y., Miyata, S., Yamada, Y., Tucker, A., Kuroiwa, T., 2012. The use of intraoperative near-infrared indocyanine green videoangiography in the microscopic resection of hemangioblastomas. Acta Neurochir. 154, 1407–1412 discussion 1412.

Tate, M.C., 2015. Surgery for gliomas. Cancer Treat. Res. 163, 31–47. Ulrich, A.S., 2002. Biophysical aspects of using liposomes as delivery vehicles. Biosci. Rep. 22, 129–150.

Vahrmeijer, A.L., Hutteman, M., van der Vorst, J.R., van de Velde, C.J., Frangioni, J.V., 2013. Image-guided cancer surgery using near-infrared fluorescence. Nat. Rev. Clin. Oncol. 10, 507–518.

Yi, X., Wang, F., Qin, W., Yang, X., Yuan, J., 2014. Near-infrared fluorescent probes in

cancer imaging and therapy: an emerging field. Int. J. Nanomedicine 9, 1347–1365.

Zehri, A.H., Ramey, W., Georges, J.F., Mooney, M.A., Martirosyan, N.L., Preul, M.C., Nakaji, P., 2014. Neurosurgical confocal endomicroscopy: a review of contrast agents, confocal systems, and future imaging modalities. Surg. Neurol. Int. 5, 60.

III. *In vivo* evaluation of photodynamic therapy using LP-iDOPE

1. Goal

In the previous chapter, we designed and developed LP-iDOPE which is a liposomally formulated phospholipid-conjugated ICG, and confirmed with fluorescence imaging that LP-iDOPE accumulated in tumor tissue for a rat glioma model. We are interested in producing ICG derivatives with phospholipid moiety resulted in new linkers for anchoring ICG fluorophore to the liposome.

In this chapter, we evaluate the efficacy of photodynamic therapy (PDT) when using LP-iDOPE *in vivo*. We carried out LP-iDOPE administration and NIR irradiation for rat glioma models and observed the longitudinal tumor growth using MRI.

2. MATERIALS & METHODS

2.1. Liposome

LP-iDOPE was prepared as previously reported (A. Suganami et al., 2015 Dec 30). Cholesterol (1.0 mM, Nippon Fine Chemical Co., Ltd., Tokyo, Japan), 1,2-dioleoyl-sn-glycero-3-phosphocholine (DOPC, 9.1 mM, NOF Corporation, Tokyo, Japan), N-(carbonyl- methoxypolyethyleneglycol 5000)-1,2-distearoly-sn-glycero-3-phosphoethanolamine sodium salt (DSPE-PEG, 0.5 mM, NOF Corporation), and iDOPE (0.9 mM, iDOPE/DOPC molar ratio of 1/10) were dissolved in a mixed organic solvent consisting of CH3OH/CHCl3 (volume ratio: 1/9).

2.2. Cells

9L gliosarcoma cell lines originating in rat were cultured in DMEM (D5796, Sigma-Aldrich Japan, Japan) supplemented with 10% FCS and 1% Penicillin and streptomycin in a humidified atmosphere of 5% CO_2 at 37˚C.

2.3. Animal models

Male Fisher 344 rats (150-200 g, 8-9 weeks old, n = 23, CLEA Japan, inc., Tokyo, Japan) were used. The animals were anesthetized with 2.0% isoflurane and placed in a stereotaxic apparatus (SR-5R, SM-15R, Narishige group, Japan). A burr hole in the skull was made at 1 mm anterior to bregma and 3.5 mm right of the midline. A 30-gauge needle was inserted to a depth of 3.0 mm ventral from the dura. The 9L tumor cells (1×10^5 in 2μL medium) were slowly injected into the brain (Iwadate et al., 2005). This animal experiment was performed in accordance with the guideline for the proper care and use of laboratory animals, and law No. 105 and notification No. 6 of the Japanese Government.

2.4. NIR irradiation device

The NIR irradiation device (DVL-20, Asuka medical INC, Japan) was connected to a probe (E400S-PL, Fuji SLI, Japan) via an optical fiber. The tip of the irradiation probe was cone-shaped to scatter NIR light. A single wavelength of 808 nm was used (Fig. 1).

2.5. Optimization of NIR irradiation power

To optimize the NIR irradiation condition for rats, ten days after the implantation of 9L cells, rats were randomly divided into 4 groups to receive different levels of irradiation strength: 1.0 Watt (W), 1.5 W, 2.0 W and a non-irradiation group as a control. LP-iDOPE (14.0 mg/kg) was injected into a tail vein, and gadolinium-enhanced MRI was acquired 24 hours after the injection. A NIR irradiation probe was inserted into the brain of an animal firmly held in a stereotactic apparatus with MRI-guidance, and NIR irradiation was applied at the selected strength. The LP-iDOPE injection and NIR irradiation was repeated 2 weeks later, after which body weight and tumor volume were mesured.

We used laser light of wavelength 808 nm, which is absorbed by LP-iDOPE. The total calorific output was 240 J for each application. The irradiation was repeated in a 500 msec on 500 msec off pattern to avoid heat damage of the tissue.

2.6. Treatment for glioma rats

Rats (n = 16) were divided into 4 different treatment strategies consisting of (1) LP-iDOPE + NIR (n = 5), (2) LP-iDOPE alone (n = 3), (3) NIR alone (n = 3), and (4) saline control (n = 5) groups. Two days after the 9L cell implantation, LP-iDOPE (14.0mg/kg, LP-iDOPE + NIR and LP-iDOPE groups) or saline (NIR and saline control groups) was administered to the rats through a tail vein (day 0). NIR light was only applied to the LP-iDOPE + NIR and NIR alone groups. Gadolinium-enhanced MRI was obtained to check localization and volume of the tumor in the brain before treatment 24 hours after the LP-iDOPE or saline administration (Fig. 2). An NIR irradiation probe

was inserted into the brain as described in Section **2.5.** The tip of the probe was placed on the upper boundary of the tumor with guidance provided by MRI.

2.7. **MRI measurement**

To evaluate the tumor volume longitudinally, MRI was measured for all animals every 7 days (Fig. 3). Rats were anesthetized with 2% isoflurane (Pfizer japan inc., Japan) and injected with meglumine gadoterate (220~280mg/kg i.p., Gd-DOTA, Magnescope®, Guerbet Japan inc., Japan, 0.283 g/ml) to enhance the glioma. Images were acquired with a 7-T animal MRI system (Magnet: BioSpec 70/20 U SR, Bruker, Germany, Console: Bruker Biospin, Germany). Tumor volume was calculated from T1W images as the Gd-DOTA-enhanced area across all slices using image analysis software (Osirix®, Pixmeo, Switzerland).

2.8. Immunohistology

After MRI acquisition, the rats were deeply anesthetized and perfused through the ascending aorta with 4% paraformaldehyde. After euthanization, the brains were carefully removed for pathological assessment. Frozen tissue sections of the brain specimens 10 μm thickness were prepared for anti-CD8 antibody and macrophage (RM-4) staining.

3. RESULTS and DISCUSSION

3.1. Optimization of NIR irradiation

LP-iDOPE was injected into the tumor bearing rats and they were NIR irradiated 24 hours later and then again after 2 weeks. We measured the body weight and MRI longitudinally for each group: 1.0 W group (n = 2), 1.5 W group (n = 2), 2.0 W group (n = 2), and non-irradiation group (n = 1).

Figure 4 shows longitudinal body weight alteration. For the 2.0 W group, two rats (2/2) died during the second opplication of the NIR irradiation. The body weight showed a descending trend for the 1.0 W, 2.0 W and non-irradiation groups from approximately 3 weeks after the implantation. On the other hand, body weight for the 1.5W group showed an graduall increase. Longitudinal MR images are presented in figure 5. A typical image for the 1.5W group at day 28 showed high contrast that is thought to be the necrotic region of the tumor. From these results, we decided to use an irradiation strength of 1.5 W with total heat energy of 240 J. The irradiation cycle was for 1 sec (exposure time: 300 msec, interval time :700 msec) and the irradiation was repeated 600 times. The total required time was 10 min.

3.2. Longitudinal evaluation of tumor volume with MRI measurement

Tumor volume before irradiation (day 1) was 0.9 ± 0.29 mm^3. The small tumor is a model for tumor that may remain but be invisible after the surgery. Figure 6 shows the longitudinal tumor progression for each group. At Day 29, tumor volume for the LP-iDOPE + NIR irradiation group was 299.0 ± 154.9 mm^3 (n = 5), for the LP-iDOPE

alone group was 337.1 ± 97.8 mm^3 (n = 3), for the NIR irradiation group was 418.5 ± 55.8 mm^3 (n = 3), and for the saline control was 307.8 ± 125.0 mm^3 (n = 5). The average tumor volume of the LP-iDOPE + NIR group was the smallest, however there was no significant difference with the other groups due to the large dispersion. Note that one animal in the LP-iDOPE + NIR group showed drastic therapeutic efficacy (Fig. 6, red dot).

3.3. Immunohistology

In the RM-4 staining, the invasion of many macrophages was observed for the LP-iDOPE + NIR group, but not for the NIR irradiation or saline control group (Fig. 7). In the anti-CD8 staining, $CD8^+$ T cells were observed not only for the LP-iDOPE + NIR group but also for the other groups. The results suggest that the combination of LP-iDOPE with NIR irradiation induced migration of macrophages. On the other hand, the migration of CD8 positive cells, which are killer T cells, was not affected by the treatment strategy. It is possible that the migrated macrophages induced for the LP-iDOPE + NIR group may activate the killer T cells and promote a tumor suppressive effect.

4. Conclusion

We evaluated the therapeutic effect of PDT using LP-iDOPE for an *in vivo* rat glioma model. A NIR strength of 1.5W was found to be best for the PDT as the body weight was unaffected by irradiation. The average tumor volume for the LP-iDOPE + NIR

group was smallest, but there was no significant difference between the other groups due to the large dispersion. For the LP-iDOPE + NIR irradiation group. Macrophages were observed, but not for the other groups. The LP-iDOPE + NIR group had a large dispersion in therapeutic effect, with one animal showing a drastic therapeutic efficacy. It is thought that further optimization of the irradiation parameters for our image-guided approach will improve the treatment effect.

References

Iwadate, Y., Inoue, M., Saegusa, T., Tokusumi, Y., Kinoh, H., MamoruHasegawa, . . . Shimada, H. (2005). Recombinant SendaiVirusVector Induces Complete Remission of Established BrainTumors through Efficient Interleukin-2 Gene Transfer inVaccinated Rats. *Clin Cancer Res, 11(10)*, 3821-3827.

Suganami, A., Iwadate, Y., Shibata, S., Yamashita, M., Tanaka, T., Shinozaki, N., . . . Tamura, Y. (2015 Dec 30). Liposomally formulated phospholipid-conjugated indocyanine green for intra-operative brain tumor detection and resection. *Int J Pharm, 496*(2), 401-406. doi:10.1016/j.ijpharm.2015.10.001

Suganami, A., Toyota, T., Okazaki, S., Saito, K., Miyamoto, K., Akutsu, Y., . . . Tamura, Y. (2012 Dec 15). Preparation and characterization of phospholipid-conjugated indocyanine green as a near-infrared probe. *Bioorg Med Chem Lett, 22(24)*, 7481-7485.

Fig. 1. The NIR irradiation device (Left image: DVL-20, Asuka medical INC, Japan) was connected to a probe (E400S-PL, Fuji SLI, Japan) via an optical fiber. The tip of the irradiation probe was cone-shaped to scatter NIR light. The irradiating light had a single wavelength of 808 nm.

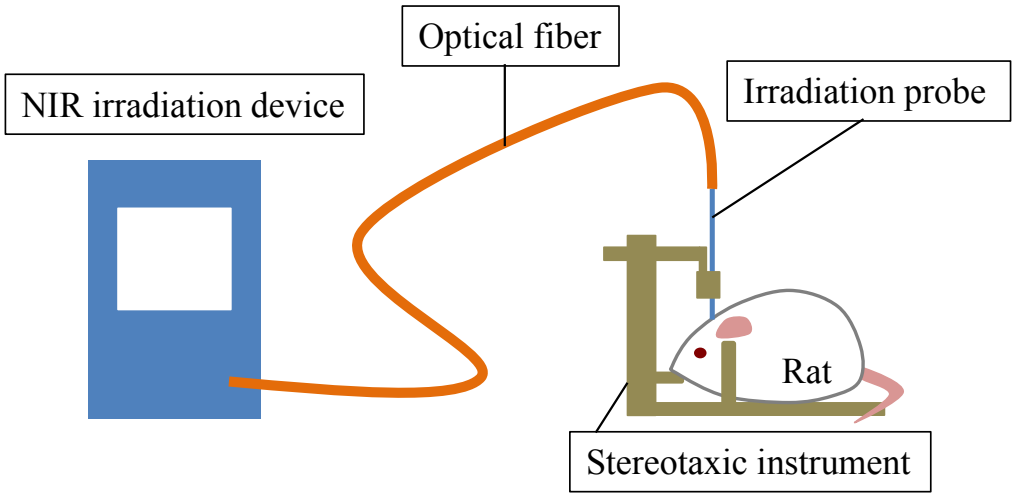

(a)

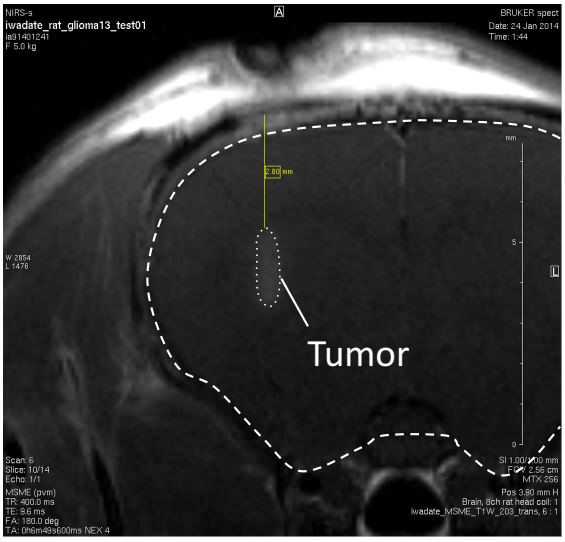

(b)

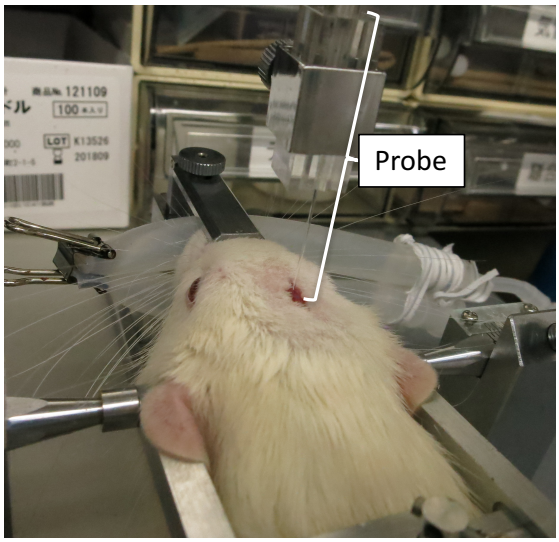

Fig. 2. Treatment: (a) Gadolinium-enhanced MRI was obtained to check the tumor localization and volume in the brain 24 hours after the LP-iDOPE or saline administration. (b) An irradiation probe was inserted in to the brain guided by MR images. NIR irradiation condition: wavelength was 808 nm, output was 1.5W, The irradiation cycle was for 1 sec (a 300 msec on 700 msec off) was repeated 600 times.

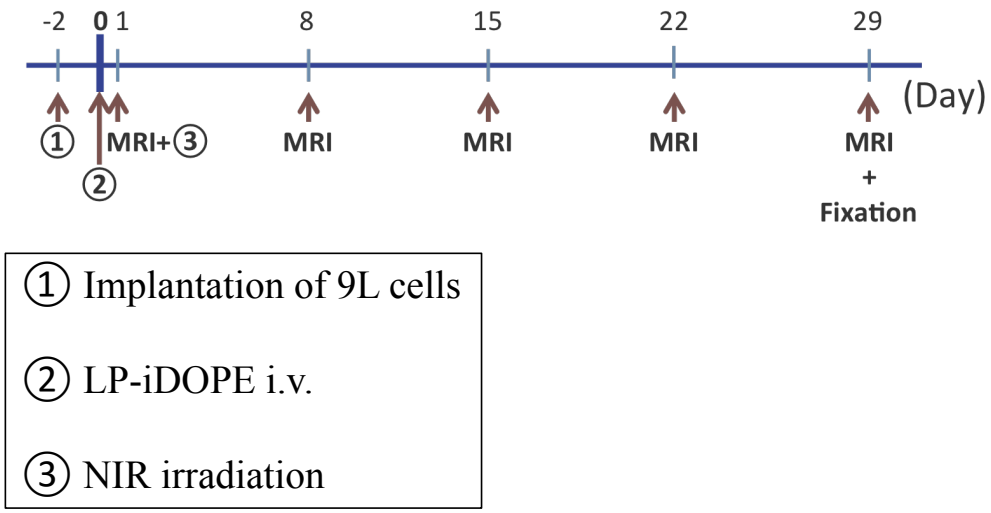

Fig. 3. Time Course of Treatment. Day 0: Two days after the 9L cell implantation, LP-iDOPE (14.0mg/kg) or saline was administered to the rats through a tail vein. Day 1 : NIR irradiation. Day 1 to 29 : To evaluate the tumor volume longitudinally, magnetic resonance imaging (MRI) was measured for all animals every 7 days.

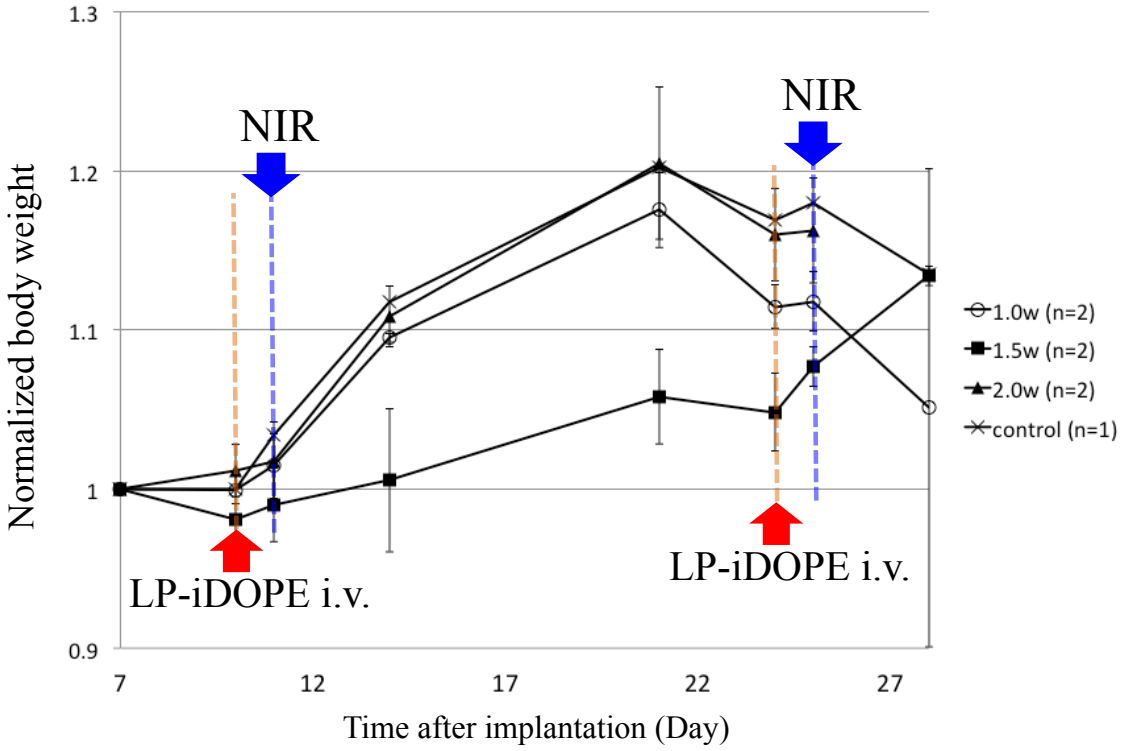

Fig. 4. Longitudinal body weight alteration. Both rats from the 2.0W group died during the the second application of the NIR irradiation. The body weight showed a descending trend for the 1.0 W, 2.0 W and non-irradiation groups, from approximately 3 weeks after the implantation.

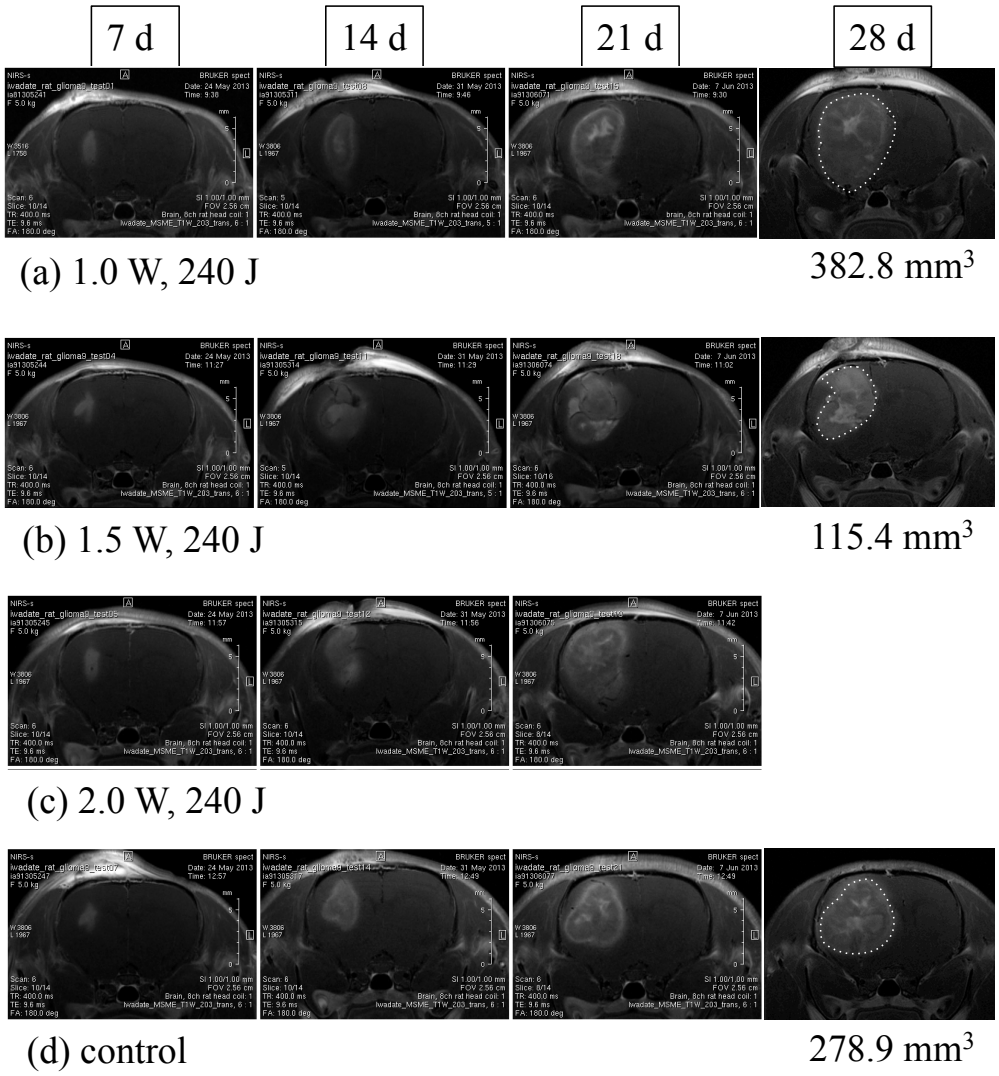

Fig. 5. Longitudinal MR images for each group; (a) 1.0 W group, (b) 1.5 W group, (c) 2.0 W group, and (d) non-irradiation group.

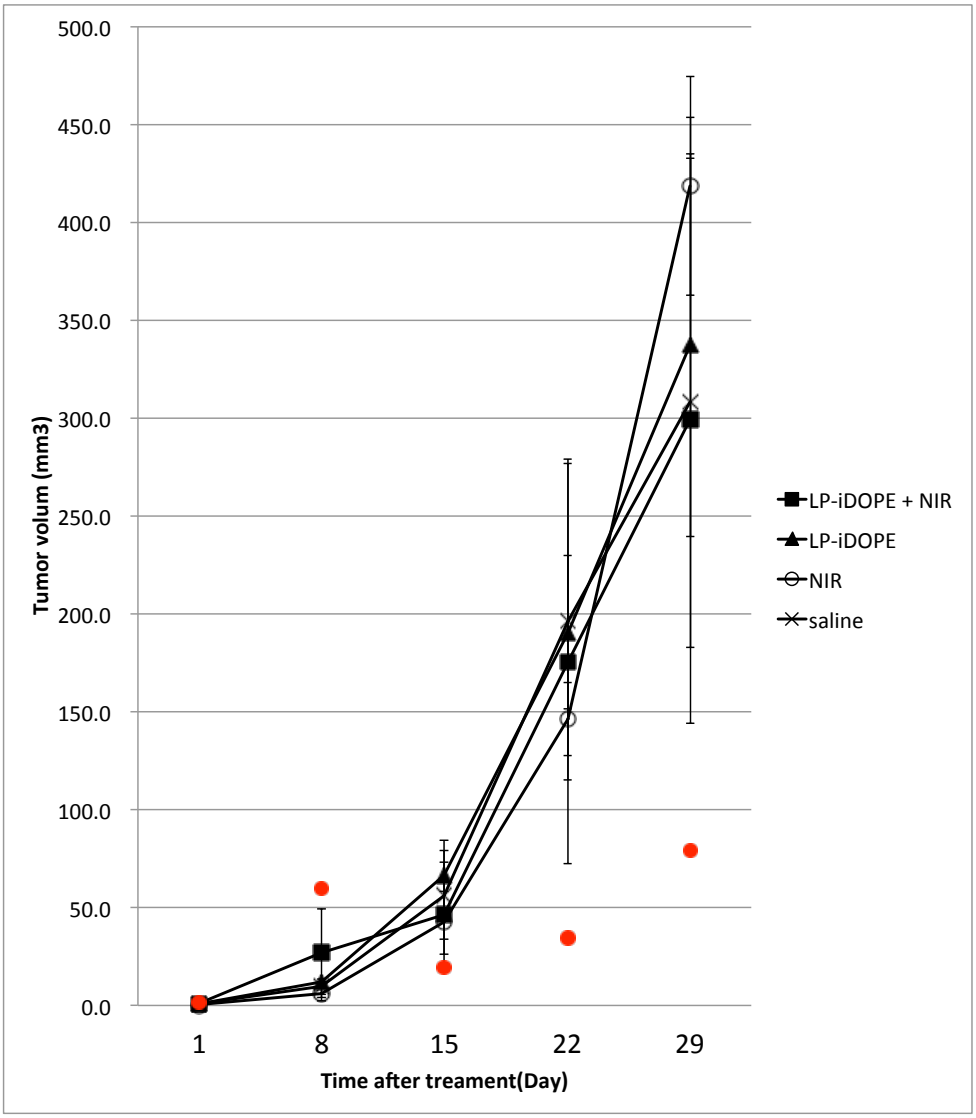

Fig. 6. Longitudinal tumor progression for each group. No significant difference occurred between the groups due to the large dispersion. Note that one animal in the LP-iDOPE + NIR group showed drastic therapeutic efficacy (red dot).

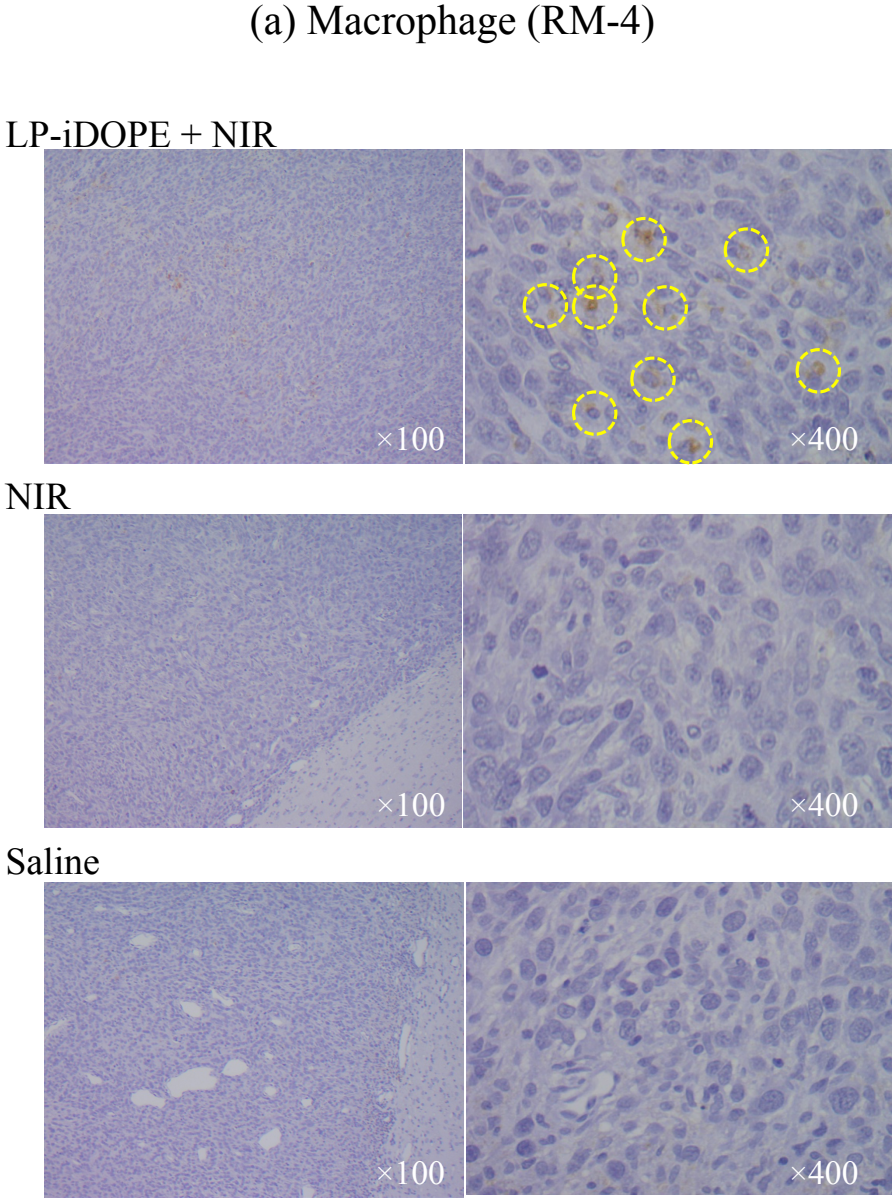

Fig. 7. Results of immunostaining i.e. (a) Macrophage (RM-4) . Diaminobenzidine (DAB) stains macrophages brown.

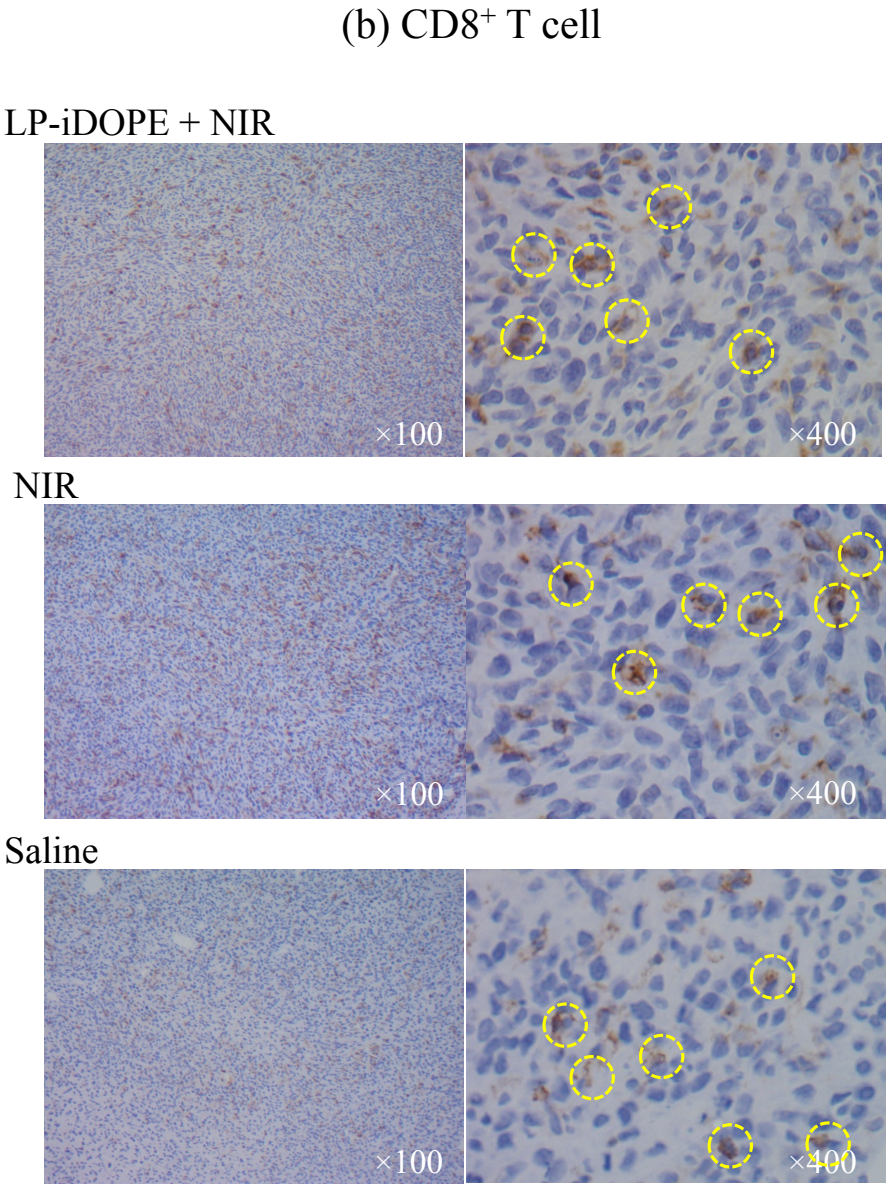

Fig. 7. (b) $CD8^+$ T-cells were stained brown by Diaminobenzidine (DAB).

IV. Conclusion

To realize our proposed theranostics concept, we first evaluated the use of liposomally formulated phospholipid-conjugated ICG, denoted by LP-iDOPE, as clinically translatable fluorescent nanoparticles for brain tumor surgery. We tested the characteristics of LP-iDOPE relevant to its use as a NIR fluorescence imaging dye, such as its optical properties, particle size, and tumor-specific accumulation. LP-iDOPE imaging with MRI and a NIR fluorescence imager, with a LP-iDOPE injection 1 day before surgery, effectively fills the gap between pre-operative imaging and intra-operative reality in detecting tumor and normal brain tissues.

Second, we evaluated the therapeutic effect of the PDT using LP-iDOPE *in vivo*. We administered LP-iDOPE and evaluated the compared NIR irradiation effect for rat glioma models. We found that a NIR intensity of 1.5W was best for the PDT. Tumor volume of the LP-iDOPE with NIR irradiation group was the smallest on average and many macrophages were observed. Although the LP-iDOPE with NIR irradiation group had large dispersion of the therapeutic effect, one animal showed drastic therapeutic efficacy. Further optimization of the image-guided approach will improve the PDT effect for LP-iDOPE strategies.

In addition to the LP-iDOPE with NIR irradiation strategy, we tried to develop two MRI sensor contrast agents for theranostic applications. First, we reported a methodology that enables the preparation of dendrimeric contrast agents sensitive to Ca^{2+} when starting from the monomeric analogue (Chem Commun (Camb). 2015 Feb 18;51(14):2782-5). The Ca-triggered longitudinal relaxivity response of these agents is maintained even with structural changes due to synthetic transformation. The in vivo MRI studies in the rat cerebral cortex indicate that the diffusion properties of dendrimeric contrast agents have great advantages in comparison to the monomeric equivalents.

Second, using carbamoyl-PROXYL (CMP) as an MRI contrast probe we developed a novel approach for detecting minute disruptions in BBB induced by dietary cholesterol (Biochim Biophys Acta. 2011 Dec; 1810(12): 1309-16).

Gd-DTPA-enhanced magnetic resonance imaging (MRI) is a conventional method for blood-brain-barrier (BBB) permeability *in vivo*. It can visualize serious injuries of the BBB. MRI-signal dynamics, plasma cholesterol, matrix metalloproteinase (MMP-9, MMP-2), and the white blood cell profile were analyzed. For the MRI analysis, we compared brain region with surrounding area in each group.

In the surrounding area of normal diet (ND) -mice, CMP- or Gd-enhanced MRI-signal followed typical kinetics with a half-life of signal decay ($\tau(1/2)$) approximately 8 or approximately 15 min, respectively. In cholesterol diet (CD)-mice, the MRI-signal increased continuously without decay. In the brain region of ND- and CD-mice, MRI-signal enhancement was not detected with Gd-DTPA. In the brain region of

ND-mice, CMP-induced MRI-signal enhancement was negligible, while in CD-mice, it was significant ($\tau(1/2)>15$ min). Hypercholesterolemia increased the plasma levels of MMP-9 and neutrophils.

The importance of these technologies will increase to realize the precision medicine, which will allow improvement of the rate of complete recovery due to early diagnosis and treatment, improving quality of life by reducing side effects, and improved decision making for more accurate surgery planning. In the study, our motivation for the development of the technology was to improve the quality of brain surgery for tumor extraction. Glioma is one of the most difficult diseases. I hope that our effort will contribute to the development of more effective treatment methods and make incurable diseases curable in the future.

I have also contributed to the development of the following novel imaging technologies:

1. Gündüz S, Nitta N, Vibhute S, Shibata S, Mayer ME, Logothetis NK, Aoki I, Angelovski G. Dendrimeric calcium-responsive MRI contrast agents with slow in vivo diffusion. Chem Commun (Camb). 2015 Feb 18;51(14):2782-5. doi:10.1039/c4cc07540d. PubMed PMID: 25383973.
2. Koyama T, Shimura M, Minemoto Y, Nohara S, Shibata S, Iida Y, Iwashita S, Hasegawa M, Kurabayashi T, Hamada H, Kono K, Honda E, Aoki I, Ishizaka Y. Evaluation of selective tumor detection by clinical magnetic resonance imaging

using antibody-conjugated superparamagnetic iron oxide. J Control Release. 2012 May 10;159(3):413-8. doi: 10.1016/j.jconrel.2012.01.023. PubMed PMID: 22300621.

3. Leuze C, Kimura Y, Kershaw J, Shibata S, Saga T, Chuang KH, Shimoyama I, Aoki I. Quantitative measurement of changes in calcium channel activity in vivo utilizing dynamic manganese-enhanced MRI (dMEMRI). Neuroimage. 2012 Mar;60(1):392-9. doi: 10.1016/j.neuroimage.2011.12.030. PubMed PMID: 22227885.

4. Autio JA, Kershaw J, Shibata S, Obata T, Kanno I, Aoki I. High b-value diffusion-weighted fMRI in a rat forepaw electrostimulation model at 7 T. Neuroimage. 2011 Jul 1;57(1):140-8. doi: 10.1016/j.neuroimage.2011.04.006. PubMed PMID: 21504797.

International Journal of Pharmaceutics *496* (2), 401-6.

(2015) Dec 30　公表済